Heliyon 9 (2023) e12728

Contents lists available at ScienceDirect

Heliyon

journal homepage: www.cell.com/heliyon

Research article

Design and manufacture of a reinforced fuselage structure through automatic laying-up and in-situ consolidation with co-consolidation of skin and stringers using thermoplastic composite materials

I. Martín [a,*], K. Fernández [a], J. Cuenca [a], C. Sánchez [b], S. Anaya [b], R. Élices [b]

[a] FIDAMC, Foundation for the Research, Development and Application of Composite Materials, Avda. Rita Levi Montalcini 29, 28906 Getafe, Madrid, Spain
[b] AERnnova, Leonardo da Vinci 13, Parque Tecnológico de Álava, 01510 Miñano Mayor (Álava), Spain

ARTICLE INFO

Keywords:
Carbon fibres
Thermoplastic resin
Non-destructive testing
Consolidation

ABSTRACT

Thermoplastic composites can be used to construct safer and more efficient aircraft fuselage structures. They provide significant weight reduction compared to conventional metallic materials, reducing the fuel consumption of the aircraft and increasing its performance and profitability. In this study, we designed and manufactured a level 2* flat fuselage specimen. The specimen comprises 2 Ω-shaped stringers and one Z-shaped frame that were manufactured using a carbon fibre-reinforced thermoplastic material. The skin was laminated on top of the stiffeners and co-consolidated to them, eliminating the need for rivets or adhesives. The manufacturing processes of the stiffeners (press-forming) and skin (in-situ consolidation) are described herein. The quality of the manufactured specimens was evaluated through non-destructive and physical–chemical testing. The test results will serve as a reference for designing and manufacturing a level 3* curved fuselage in a future study.

*Level 2: "Element tests according to the Building Block approach (MIL-HDBK-17, 2002) [18]"; Level 3: "Detail tests according to the Building Block approach (MIL-HDBK-17, 2002) [18]".

1. Introduction

The aeronautical industry has devoted significant effort towards replacing metallic fuselages with composite fuselages, as demonstrated by the Large Aircraft Composite Fuselage (LACF) program and the Advanced Technology Composite Aircraft Structure (ATCAS) program for dual-aisle commercial aircraft. Similar improvements for single-aisle commercial aircraft are currently underway [1].

The key considerations in the development of new fuselages are achieving recurring cost and total weight reductions, and productivity rates of at least 100 aircraft/month [2]. To achieve these goals, it is essential to realise high modularity, a high rate of production, quick and clean welding processes, and significant interdisciplinary cooperation. Accordingly, thermoplastic composites are considered to be a good alternative to conventional metallic structures.

Several studies have examined the viability of using thermoplastic composites for fuselage structures; for example, TAPAS2, which

* Corresponding author.
E-mail address: maria-isabel.martin@fidamc.es (I. Martín).

https://doi.org/10.1016/j.heliyon.2022.e12728
Received 21 April 2022; Received in revised form 19 December 2022; Accepted 22 December 2022
Available online 29 December 2022

aimed to suppress fasteners between the skin and frames [3,4], and STUNNING (Smart Multi-Functional and Integrated TP Fuselage) [5].

Recently, Stelia Aerospace developed a thermoplastic composite fuselage. They presented a full-scale demo structure, wherein the skin was manufactured using automatic fibre placement (AFP) and consolidated using autoclave processes, and the stiffeners were obtained through rapid stamping.

Kothe et al. [6] examined the use of thermoplastic composites as an alternative material for future fuselage structures; this work was performed as part of the Clean Sky 2 - MultiFAL (Multifunctional Fuselage Demonstrator) program. They used thermoplastic welding technologies to bond the shell components of the fuselage. The higher material costs were compensated by the lower process costs of this method. The project is expected to achieve a technology readiness level (TRL) of TRL 6 for new materials, manufacturing, and assembly.

Significant research has been performed on technologies such as induction welding, with the aim of producing a thermoplastic fuselage structure. For example, the SIDEFFECT project, which began in 2017, aims to find a manufacturing solution that offers low costs and high speed processing.

In-situ consolidation can eliminate the secondary steps and costs of autoclave cycles and appears to be a viable alternative. It involves the addition of material tapes on top of a substrate, using a heating source to increase the temperature of the material above its melting point and a compaction roller to provide the required pressure. In-situ consolidation can be used to manufacture parts without the need for subsequent curing in an oven or autoclave. It can achieve high integration by applying co-consolidation between the skin and the reinforcements, as demonstrated by the Advanced Low Cost Aircraft Structures (ALCAS) project [7], wherein a highly integrated composite wing box was fabricated using poly-ether-ketone-ketone carbon fibre unidirectional preimpregnated material (PEKK CFRP UD) tapes.

The various factors that affect the automatic laying-up and in-situ consolidation of thermoplastic composites were discussed in Ref. [8]. To incorporate these processes at an industrial level, several limitations must be overcome: reducing the number of voids, increasing the lamination speed, controlling the residual stresses, and achieving mechanical performances that are close to those of composites processed in an autoclave.

The processing parameters, such as the heating source, heating power, heat source spots, compaction pressure, and lamination speed, have a significant impact on the mechanical performance of composites generated through in-situ consolidation. Weber and Schlimbach [9] performed a comprehensive study on in-situ consolidation, and identified the benefits of using simulation modelling to design improved solutions, such as those developed in Refs. [10,11].

Crystallisation development, not only in terms of the degree of crystallisation but also in terms of the morphology, is a key consideration in in-situ consolidation. A recent study using novel materials (low melting poly-aryl-ether-ketone (PAEK)) demonstrated that several variations can be obtained in terms of the crystallinity and single lap shear by modifying the lamination speed, nip point temperature, and tooling temperature, and by performing post-manufacturing tempering [12].

Various studies [13–15] have suggested that automatic laying-up of thermoplastic composites can be used to produce highly integrated aeronautical parts, wherein the skin is directly bonded to stiffeners by placing the composite sheets on top of the stiffeners. Bandaru et al. [16] collected information relating to the interlaminar shear strength, double cantilever beam, and end-notched flexure as mechanical testing quality criteria, and demonstrated that strong joints can be achieved through in-situ consolidation.

Most existing studies have focused on determining the capability of part production and resolving manufacturing problems. Consequently, there is an urgent need for studies that focus on the industrialisation of manufacturing processes, with the aim of achieving higher TRLs, such as in the study conducted by Veijer [17].

2. Design

A flat specimen (level two) was designed, with two main aims:

1) Verify the viability of thermoplastic materials and in-situ consolidation.

Accordingly, two fibre areal weights (194 g/m^2 and 134 g/m^2) were used and different manufacturing details (drop off, joint between frames and stringers) were analysed.

2) Perform material tests to determine the material properties, allowable structural integrity of the thermoplastic material, and design details for the (level 3) curved panel that will be manufactured in the next phase of the project (in a future study).

The panel was designed to allow the coupon and specimen extraction required for the proposed level 2 [18] test matrix:

1) Filled hole tension, open-hole compression, bearing and pull-through tests: coupons taken from skin
2) Crippling and mouse hole tests: machined specimens that include the joint between the skin, stringers, and frame
3) Unfolding and de-bonding tests: specimens that include the joint between the frame and skin.

The flat specimen was a 1 × 1 m^2 skin, reinforced with 1 Ω-shaped straight stringer, 1 Ω-shaped joggled stringer, and one Z-shaped frame, as shown in Fig. 1.

A model of the flat specimen was created using CATIA V5 R21. The Ply by Ply methodology of the Composite Part Design (CPD)

workbench was used to define the composite parts, and the Functional Tolerancing and Annotations (FTA) workbench was used to define notes, processes, and tolerances.

The design details of each component were analysed; the best design will be used for the level 3 curved panel, which will represent a fuselage panel, and will be tested in the subsequent project phase.

2.1. Stringers

Considering the stringers, an omega section was selected as the best option for the level 3 curved panel as it provides high inertia and torsional stiffness, which is beneficial for highly pressurised panels such as fuselage panels (see Fig. 2).

The stringer edge was defined as a straight vertical edge instead of an "in-ramp" edge because "in-ramp" edges are only useful for autoclave (pressurised) processes. For processes such as in-situ consolidation, which occurs outside an autoclave, a vertical edge simplifies manufacturing.

A joggle, which is typical in aircraft design, was also included to verify the processability of this geometric feature. Accordingly, two different stringers, one with a joggle and the other without a joggle (see Fig. 3), were designed herein. The figure shows the stringer base on the skin (in the area of skin with and without reinforcement plies) and the corresponding drop off.

One issue that affects the stringer design is the difference in the thicknesses of the stringer and frame bases owing to the different structural requirements of each part (Fig. 4). A machined fitting with a step in its base was designed to solve this problem (see Section 2.4).

The stringer laminate was defined with several plies in the 0° direction ("hard" laminate), where 0° is the longitudinal direction of the stringer, to provide high stiffness, strength, and stability as the stringer experiences high axial loads (see Section 5.3).

2.2. Frames

Frames are highly loaded elements that experience bending loads caused by the non-circular section of the fuselage. The frame web cannot withstand these loads and an inner chord is necessary to provide stability and stiffness under compression loads. A 'Z' section was selected for validation, considering the manufacturability criteria of the level 3 curved panel design. The dimensions of the frame section, with a length of 1000 mm, are shown in Fig. 5.

The minimum frame bending radius was set to 3.5 mm to avoid manufacturing problems (such as wrinkles) that may appear in sharp corners. The frame base width was wide enough to accommodate a fastener that was installed with the appropriate edge distance and is required for the assembly of the reinforcement fittings. To minimise the potential local buckling problems, the frame cap width was 28 mm, with a height/thickness ratio of approximately six to provide stability. As in the case of the stringers (see Section 2.1), the edge of the frame base was defined with a straight trim. The frame also required the inclusion of a joggle to adapt to the two thicknesses of the panel. The manufacturability of this geometrical configuration was verified as well (see Fig. 6).

The frame laminate was quasi-isotropic (similar quantities of fibres oriented in different directions) to facilitate manufacturing.

2.3. Skin

Considering the manufacturing process (in-situ consolidation) and the goal of validating the joggles used in the stringer and frame, a skin with a ply drop-off area (skin with two different thicknesses) was designed herein. Various alternatives were analysed for the skin reinforcement area; the selected area had the largest panel surface without any reinforcement, to extract as many testing coupons as possible. The reinforcement plies were placed along the 0/90° directions to guarantee a perfect 90° corner.

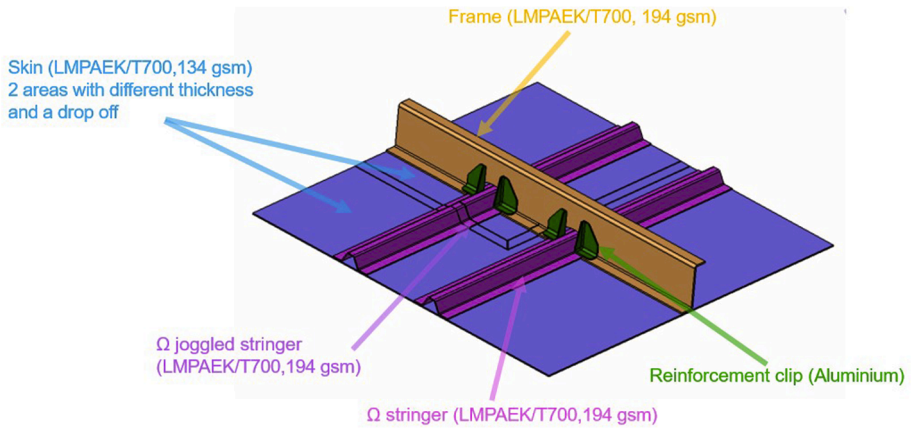

Fig. 1. Details of skin reinforced specimen: level two flat fuselage (For interpretation of the references to colour in this figure caption, the reader is referred to the web version of this paper).

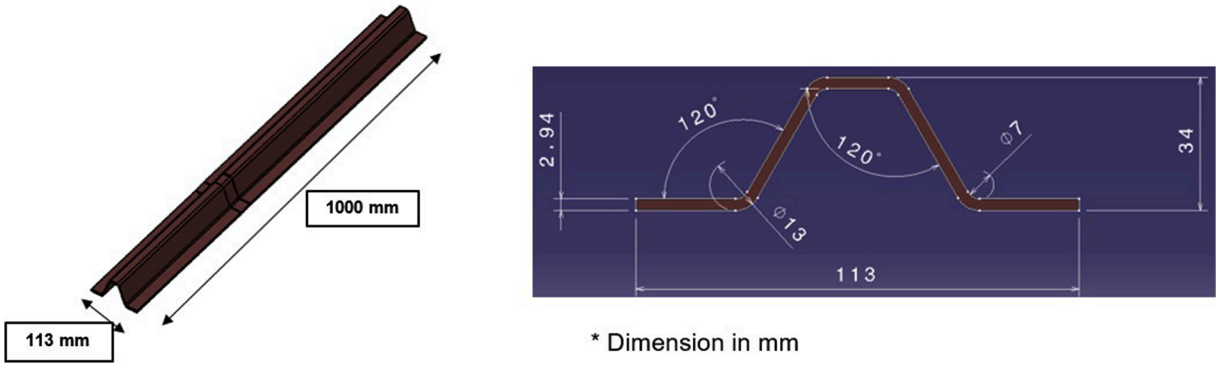

Fig. 2. Stringer dimensions (all units in mm).

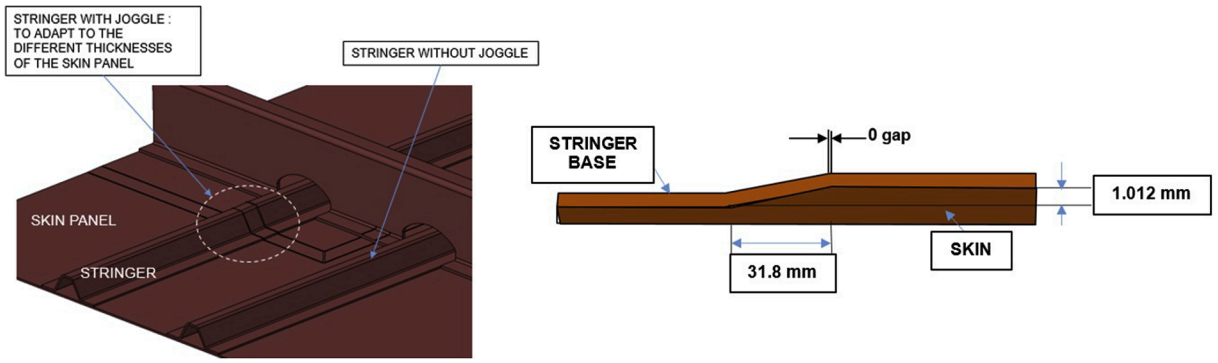

Fig. 3. Stringers with and without joggle and stringer joggle dimensions (For interpretation of the references to colour in this figure caption, the reader is referred to the web version of this paper).

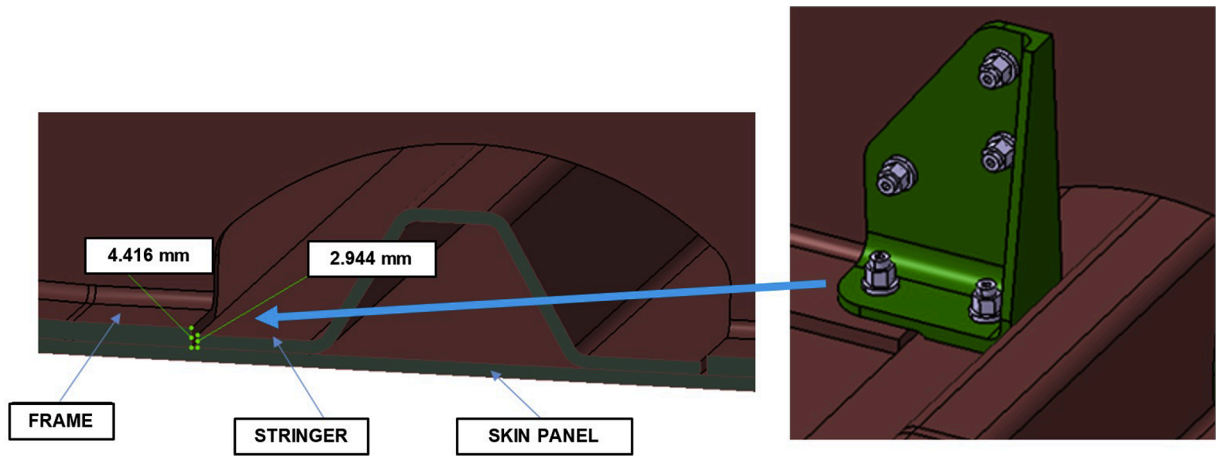

Fig. 4. Difference in thickness between frame and stringer bases (For interpretation of the references to colour in this figure caption, the reader is referred to the web version of this paper).

The general dimensions of the skin (with the two thickness) and ramp detail are shown in Fig. 7.

2.4. Reinforcement fittings (clips)

The initial analyses of the panel indicated the possibility of de-bonding problems at the frame–skin joint near the mouse holes areas (see Fig. 8).

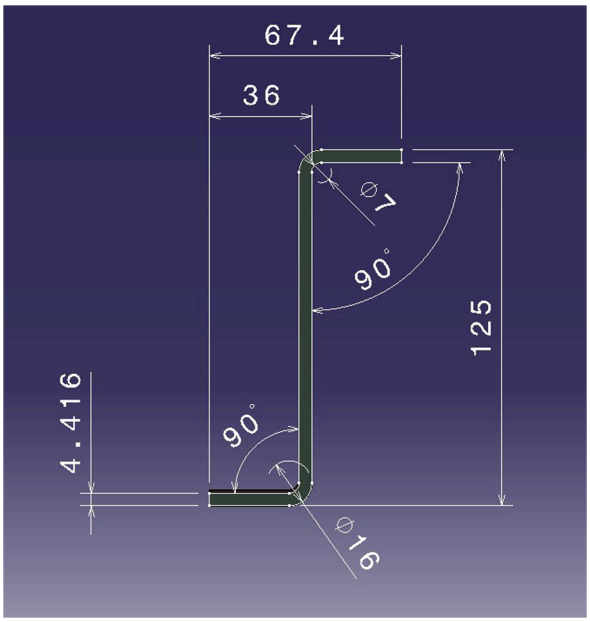

Fig. 5. Frame section dimensions (all units in mm).

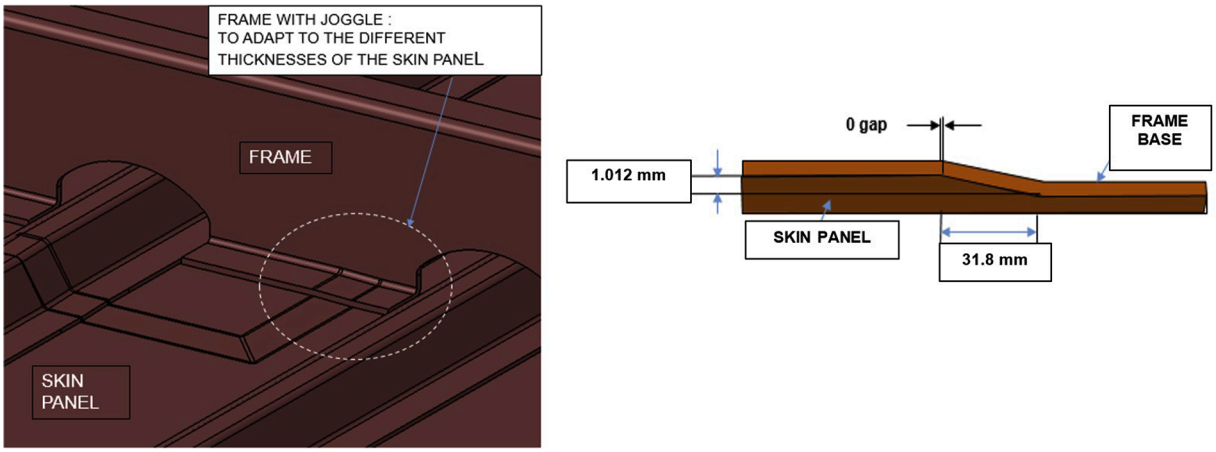

Fig. 6. Frame joggle and frame joggle dimensions (For interpretation of the references to colour in this figure caption, the reader is referred to the web version of this paper).

Stringer fittings were used to overcome the de-bonding problem. Although welded thermoplastic fittings were considered initially, it was not possible to develop them within the time frame of the project and guarantee that they would have the required quality to provide the desired failure mode during the structural tests of the curved panel. Therefore, machined aluminium fittings were designed and used instead (dimensions and material directions are shown in Fig. 9). This in an initial compromise solution to test the part, for future developments, other solutions should be considered (as thermal welding in the crossing areas).

The fittings were assembled in the 2 specimens extracted from areas 1 and 2 (shown in Fig. 10) and tested in accordance with the level 2 test matrix (mouse hole test) [18]. The fittings were riveted to the frames, stringers, and skin.

2.5. Laminates

The laminates were defined in accordance with the typical design guidelines: a minimum of 10% of the plies were oriented in each direction (0, 90, +45, −45); no more than three consecutive plies were placed in the same direction; and angles above 45° were avoided between consecutive layers.

Considering the thickness of each component in the flat specimen, we compared four different stacking sequences. Abaqus 6.13-4 was used to analyse the different configurations. The laminates were selected such that the coupling terms of the material matrix were

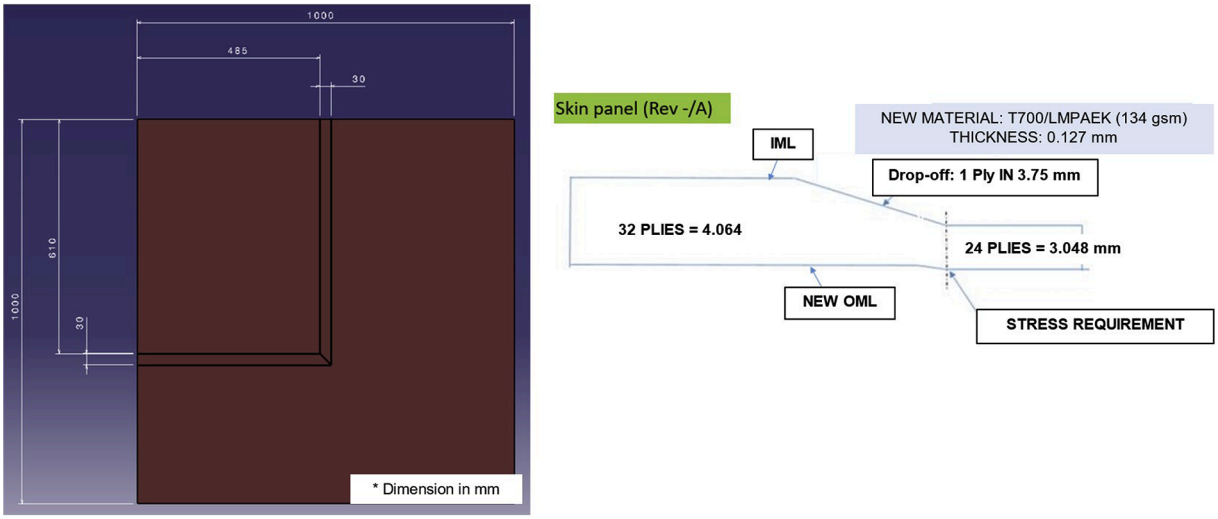

Fig. 7. Skin dimensions and ramp (For interpretation of the references to colour in this figure caption, the reader is referred to the web version of this paper) (all units in mm).

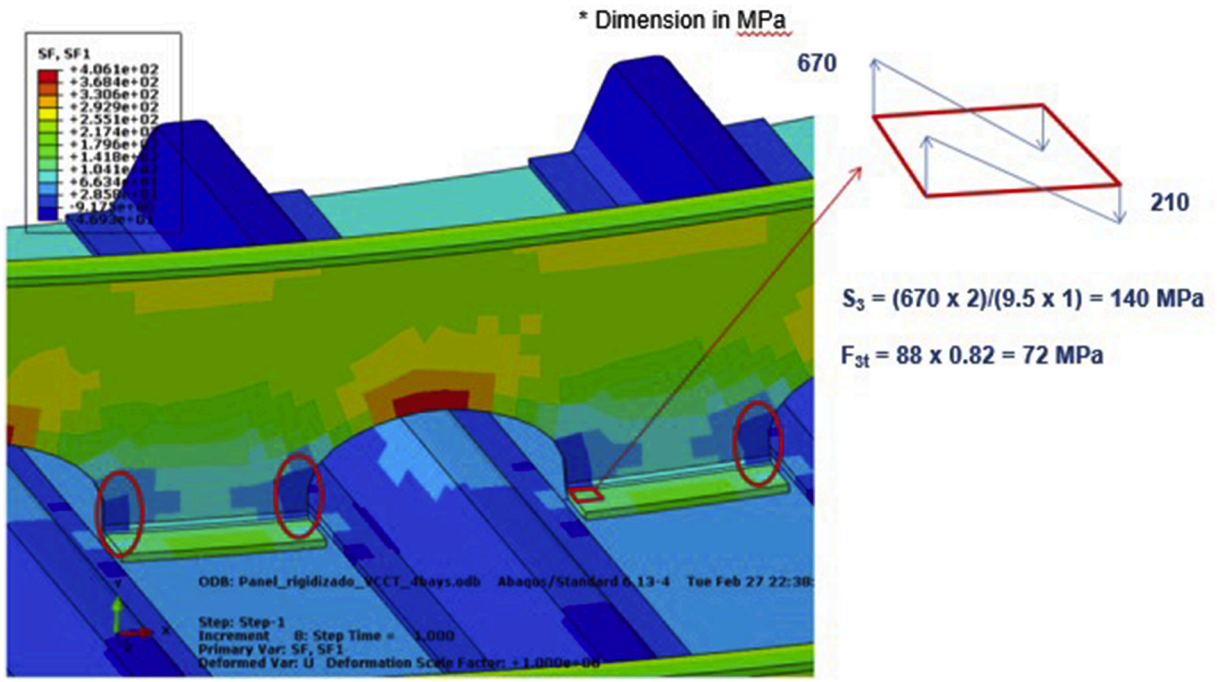

Fig. 8. Debonding at frame–skin joint in mouse hole areas (For interpretation of the references to colour in this figure caption, the reader is referred to the web version of this paper).

minimal, thereby reducing the strain level and the potential spring back effects that can be caused by the heat of the in-situ consolidation process. The final laminates and stacking sequences of each component are described in Section 5.

3. Manufacturing methods and equipment

Co-consolidation was employed during manufacturing to fabricate a highly integrated structure. It allows the skin to be directly laminated on top of the stringers, without the need for adhesives or bolted joints. The stringers, which are generated by press-forming, are positioned on the tooling and joined to the skin while it is automatically placed and consolidated.

To analyse the degree of bonding achieved when lamination is performed on top of a pre-consolidated stiffener, different tests were

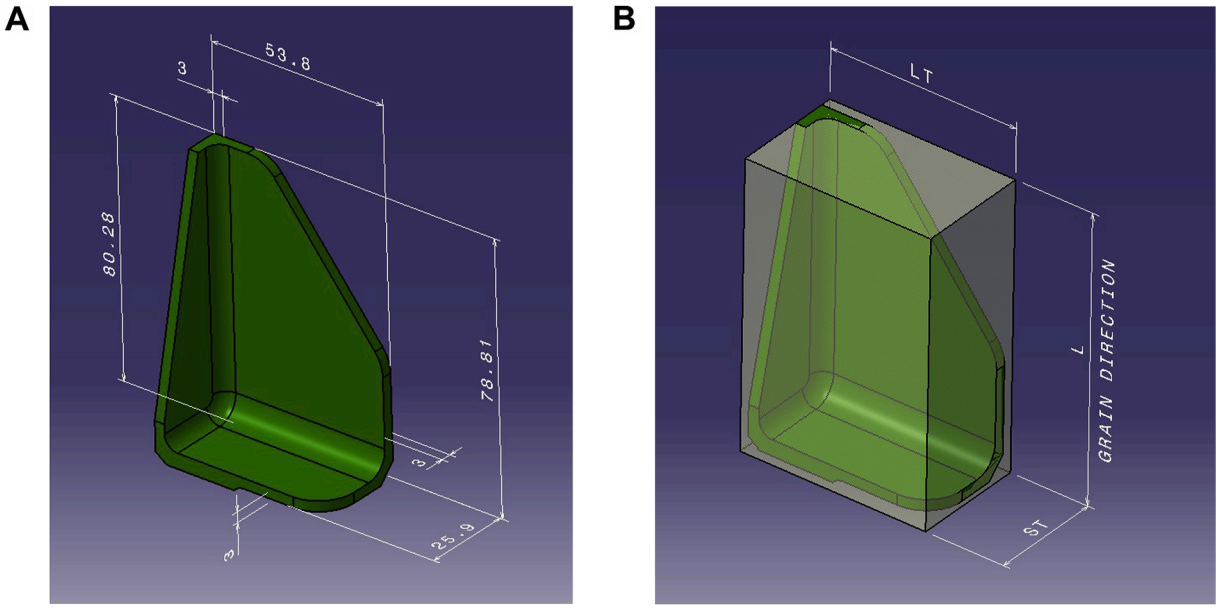

Fig. 9. Reinforcement fittings: (a) general dimensions and (b) material orientation (all units in mm).

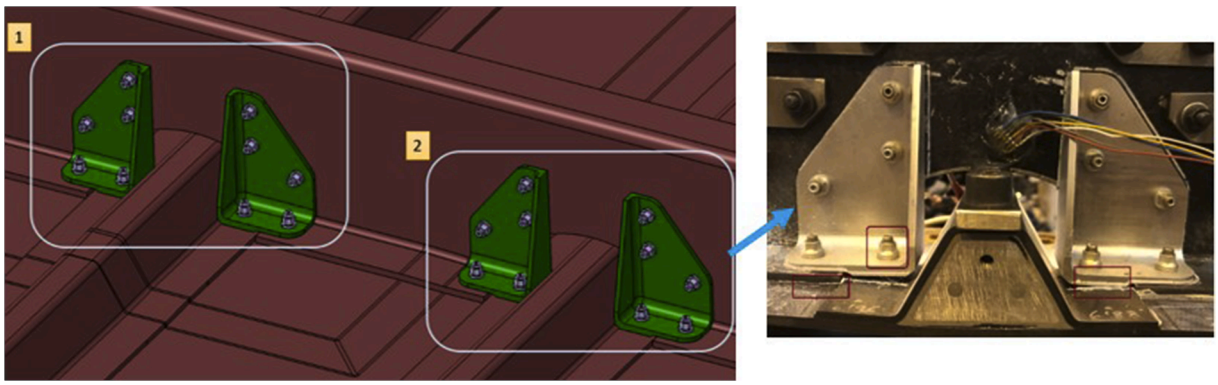

Fig. 10. Reinforcement fittings riveted in mouse hole test specimens.

performed for Mode I fracture (G_{1c}) and single lap shear (Slotted single lap shear (SLS) specimen; Test procedure A). The tests were developed in accordance with the EN 6033:2015 (G_{1c}) and EN 2243-1:2005 (SLS) standards.

To obtain coupons for the G_{1c} test, an artificial pre-crack was generated using a film of Upilex 50S placed on top of the substrate panel, which was attached to the tooling using kapton adhesive tapes (Fig. 11). Considering the SLS coupons, no insert was required to induce a pre-crack (Fig. 12). However, after manufacturing, both halves of the sample were slotted with a separation of 12.5 mm by penetrating half the thickness of each component.

In addition to these tests, which were performed in accordance with the established standards, a quasi-isotropic laminate was developed to resemble the part sequence (reinforced skin) for the G_{1c} test. This was not used for the SLS test owing to the precision required to create the slots and the lack of a reference in the bonding line (e.g., a coloured adhesive).

3.1. Materials

The components were developed using the Toray Cetex® TC1225 PAEK material, which comprises a standard modulus carbon fibre

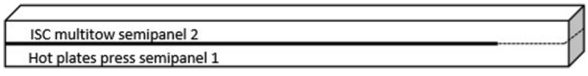

Fig. 11. G1c panel configuration.

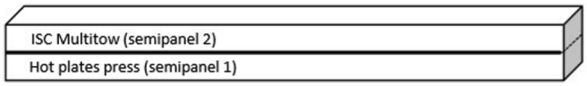

Fig. 12. SLS panel configuration pre-slots.

(T700) and semicrystalline thermoplastic matrix; the main material properties are listed in Table 1. Two different fibre areal weights were employed herein: 134 g/m^2 for the skin and 194 g/m^2 for the stiffeners.

3.2. Stiffeners

3.2.1. Equipment

A 600 × 600 mm^2 hot plate press purchased from the IDEC Corporation was used to manufacture the flat panels. The panels were placed as substrates for subsequent lamination (development of testing coupons). They were consolidated by using a metallic frame with a thickness that was 10% lower than the theoretical thickness of the panel.

A 1.5 × 1.5 m^2 hot plate press purchased from the Marzola Biele Group (La Rioja, Spain) was used for thermoforming the 'Z' frame and omega stiffeners. The system provides a maximum applied force of 1000 T and a maximum temperature of 450 °C. Owing to the limits of the closing speed (60 mm/s), a thermoforming process was employed instead of a thermo-stamping process.

3.2.2. Tooling

Three specific tools were developed, one for each geometry (omega-shaped stringer, omega-shaped joggled stringer, and Z-shaped frame), in collaboration with Fundación para la Investigación, Desarrollo y Aplicación con Materiales Compuestos (FIDAMC), Aernnova Composites Illescas (ACI), and Aernnova Engineering Division (AED). The tools were manufactured using steel alloys. A kapton film, which was treated with demoulding agents, was used to wrap the laminate before cycling.

In contrast to the omega stiffeners, which required only one press cycle, the Z-shaped frames required a double press cycle process. The first is a forming cycle and the second is a consolidation cycle that attempts to distribute the pressure not only through the head and foot of the frame, but also through the web. Two different tools were developed for this purpose.

3.3. Skin

3.3.1. Equipment

The upper half of the test panels, which was used to evaluate the interface, were developed in the same manner as the demo skin, using a gantry-style multiple-tow lamination machine developed by MTorres (Pamplona, Spain) that simultaneously places 6 tows, each with a ¼-inch width.

The selected lamination speed was 1 m/min, which was determined from preliminary trials that examined the benefits of in-situ consolidation by comparing the mechanical test results of in-situ consolidated composites with those manufactured using an oven or press.

3.3.2. Tooling

The lamination tooling comprises a self-heated component with an interchangeable chassis that can be used for horizontal or vertical lamination (can potentially be used if attached to a mandrel). As lamination is performed at a surficial temperature of 180 °C, the thermal expansion of the metallic modules and the entire table was considered at the design stage.

The tooling temperature was determined from preliminary trials. Based on bibliographic research [19] and mechanical tests performed on samples that were laminated at different tooling temperatures, a temperature of 180 °C was selected as the optimal condition.

The tooling incorporates housing areas to position the stiffeners and metallic modules, as shown in Fig. 13. The tooling material—except for the metallic modules, which were manufactured using a beryllium–copper alloy for thermal stability purposes—was steel.

The thermal stability and homogeneity of the tooling were examined before starting the lamination process by placing the stiffeners and metallic modules, and attaching thermocouples to the surface, as shown in Fig. 13. A thermal variation of 20–50 °C was observed

Table 1
General properties of LMPAEK.

Property	Value
Nominal Consolidated Ply Thickness (TC1225 194 g/m^2) mm	0.185
Nominal Consolidated Ply Thickness (TC1225 134 g/m^2) mm	0.128
Nominal resin content (%)	34
Glass Transition Temperature (°C)	147
Melt temperature (°C)	305
Typical processing temperature (°C)	340–385

between the metallic modules and stiffeners and the other lamination areas (from higher to lower temperature: skin lamination area, stiffeners and metallic modules). This temperature difference directly impacts the lamination process because the power demand is conditioned by the heat flow across the table and so generating heterogeneities in the part manufactured, a variable degree of bonding. The positioning tolerance is another critical consideration, as subtle variations in height compared to the rest of the lamination area may be required to compensate for the vertical displacement of the machine.

4. Quality evaluation

Non-destructive inspections were performed using ultrasound equipment to verify the quality of the reference flat panels and the stiffeners after press-forming. Subsequently, a global inspection of the skin attached to the stiffeners was performed as well.

The flat panels used to establish the lamination conditions were analysed both physically and chemically by evaluating the degree of crystallisation and void content, and by performing a microscopic analysis. In-plane shear strength tests were performed to evaluate the mechanical performance.

Several samples were extracted from the panel growth areas in the skin–stiffeners demonstrator to analyse the crystallinity levels and for optical inspections.

4.1. Equipment

Two pieces of equipment were used for the non-destructive inspection: an Epoch 650 ultrasonic detector and an automated Triton 8000 TT + equipment supplied by Tecnitest (Spain).

The degree of crystallinity was analysed through differential scanning calorimetry (DSC), using a calibrated Q2000 DSC coupled with a refrigerated cooling system (RCS) from TA Instruments. The tests were performed in accordance with ISO 11357-3 [20]. The crystallinity was calculated using Eq. (1).

$$X = \frac{\Delta H_m - \Delta H_c}{\Delta H_f (1 - \alpha)} \tag{1}$$

where ΔH_m is the enthalpy of fusion at the melting point, ΔH_c is the enthalpy of cold crystallisation, ΔH_f is the enthalpy of the completely crystalline polymer (estimated as 130 J/g), and α is the carbon fibre weight fraction.

The void content was measured by employing acid digestion, in accordance with EN 2564 [21].

Microscopic analyses of the flat panels and the stiffened demonstrator were performed using an Eclipse LV150 microscope manufactured by Nikon. The samples were polished and subsequently observed using a Phoenix 4000, Buehler GmbH. The characterisation was performed in accordance with AITM 4-0005 [22].

5. Results

The results included in this section are based on the analysis of the quality of each component manufacturing: how to improve quality of lamination with LMPAEK, how to obtain good quality in manufacturing the stringers and how to develop co-consolidation of skin plus stiffeners with the best consolidation and bonding levels. No information is included here regarding the behaviour of the final part. Mechanical testing of this element belongs to a second phase of the project which contains: flat panel testing for curved geometry

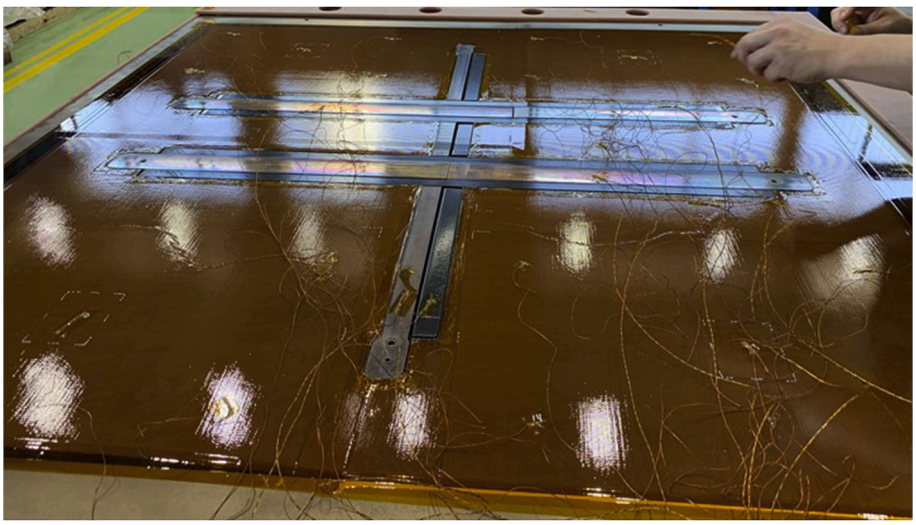

Fig. 13. Lamination tooling with modular structure housing the stiffeners.

definition and curved panel manufacturing and testing under typical fuselage loads.

5.1. Flat laminates

Several trial specimens were developed using the in-situ consolidation method using both LMPAEK material grades. Compared to the 134 g/m^2 material, the 194 g/m^2 material exhibited a lack of consolidation, with poor quality and insufficient in-plane shear strength. Therefore, the skin was designed using the 134 g/m^2 material and optimised to fulfil the loading requirements. The in-plane shear strength results and physical–chemical characterisation of the flat panels manufactured through in-situ consolidation using the 134 g/m^2 material are listed in Table 2, which also compares the influence of two different tooling temperatures. A temperature of 180 °C improved both the mechanical performance and crystallinity, which are used to define the required tool temperature for the manufacturing described in the following subsections. The increase in void content is negligible and remains in the range allowed by the standard requirements (there are many effects associated to the increase in tooling temperature for in-situ consolidation processes that could slightly increase the void content without a noticeable impact in mechanical properties, for example the reduction of thermal residual stresses. This consideration is different for oven panels, where effects as thermal residual stresses are not as notorious). The strength of the prepared panel was approximately 75% of that of a reference panel manufactured in an oven (Table 3).

5.2. Interface evaluation of flat laminates

The results of the G_{1c} and SLS tests on the panels are presented in Table 4 (two panels for each test and developed under same manufacturing conditions, 6 coupons extracted per panel) and Table 5. The panels were inspected using non-destructive testing, fulfilling the 6 dB limit criteria.

5.3. Stiffeners

Both the omega stiffeners were composed of laminates containing 16 layers with the sequence $[+45, 0, -45, 90, -45, 0, 45, 0]_s$. In accordance with the supplier instructions, the material was heated to 365 °C and maintained at this temperature for several minutes. Their position in the demonstrator is shown in Fig. 14.

Considering the omega-shaped stiffeners, after verifying that the carbon fibres can maintain stability without breaks, the two halves of the tooling were kept shut from the beginning of the cycle (at room temperature) with the material inside to ensure a proper temperature distribution. Thermal control of the cycle was performed using J-type thermocouples that were embedded among the layers of the composite material. The measurements of the thermocouples were directly passed to the control system of the press. Once the stabilisation temperature was reached, the set point pressure was automatically applied by the equipment.

During the cooling stage, both halves of the tooling were kept closed until the interior temperature was below the glass transition temperature of the material. Final demoulded parts (straight and joggled omega) are included in Figs. 15 and 16.

Considering the Z-shaped frame, a double cycle process was used herein. Compared to the omega-shaped stiffeners, the Z-shaped frame was composed of 24 layers with the stacking sequence $[45, 0, -45, 90, 45, 0, -45, 90, 45, 0, -45.35, 90]_s$. Owing to the increased thickness of the component, the strategy applied to the omega-shaped stiffeners could not be applied to the Z-shaped frame; that is, the two halves of the tooling could not be closed from the beginning of the cycle. For the first cycle, the material was clamped using a screwed platen in a cantilevered state. When the thermocouples attached to the laminate measured the required temperature, the automatic control of the press closed both parts to form the required shape. The tooling closure was controlled by gauges to control the thickness of the part. For the second cycle, the tooling orients the part at a 45° rotation angle to allow pressure application over the frame web; the pressure was directly applied to the laminate. Final demoulded part is shown in Fig. 17.

5.3.1. Skin

The skin is a 1 × 1 m^2 component with 24 layers, and a reinforced corner area with 32 layers. The stacking sequence in the non-reinforced area was $[45, 0, -45, 90, -45, 0, 45, 90, -45, 0, 45, 90]_s$ and that in the reinforced area was $[45, 0, -45, 90, 90, -45, 0, 0, 45, 90, 90, -45, 0, 0, 45, 90]_s$. The laminated reinforced layers are visible in the bottom left corner of Fig. 18.

The first layer was placed using the hand lay-up technique and one laser repass was applied to ensure its adhesion with the stiffeners. The last two layers were also repassed to increase the final degree of bonding, as suggested in Ref. [23].

To control the temperature during the process, FIDAMC developed an automatic system that measures the temperature using a thermographic camera (as shown in Fig. 19) and generates a response based on several pre-determined conditions (required temperatures, thresholds, and control areas). This system uses a closed loop architecture featuring a proportional–integral–derivative (PID) controller. Other control alternatives such as direct power or speed versus power profiles can be used as well. The PID system was used for lamination of the frame in the Clean Sky Large Passenger Aircraft (LPA) project, exhibiting a highly stable response. The part was laminated at a set point of 380 °C at the nip point (the point just before the contact between the incoming tow and substrate). The other lamination parameters are listed in Table 6. Most of them are based on previous experience working with this technology and in thermal simulations that are out of the scope of this research.

The software also retains other information relating to the lamination process, such as the power evolution, temperature, and lamination speed, and stores a large amount of data.

The main problem with this configuration is the heatsink effect detected in the metallic modules that interact with the stiffeners; Fig. 20 represents the crossing area with the frame foot and Fig. 21 represents the crossing area with the omega feet. The large thermal

Table 2
Test results of 134 g/m^2 LMPAEK in-situ consolidated panels.

Panel sequence	Tooling temperature (°C)	IPSS strength (MPa)	IPSS modulus (GPa)	Crystallinity (%)	Voids (%)
[0/90]4s	160	157 ± 3	3.73 ± 0.1	21.3 ± 0.1	0.9 ± 0.1
[0/90]4s	180	176 ± 1.2	3.73 ± 1.2	28.9 ± 3.7	1.2 ± 0.0

Table 3
Test results of 134 g/m^2 LMPAEK panels prepared in an oven.

Panel sequence	IPSS strength (MPa)	IPSS modulus (GPa)	Crystallinity (%)	Voids (%)
[0/90]4s	236 ± 4	3.99 ± 0.1	25.5 ± 4.5	0.2 ± 0.1

Table 4
G_{1c} and SLS results of 134 g/m2 LMPAEK panels (standard laminates).

Panel sequence	G_{1c} [J/m^2]	Panel sequence	SLS [MPa]
$[0]_{12}/[0]_{12}$	1298 ± 135	$[0]_{16}/[0]_{16}$	38.18 ± 2.62
$[0]_{12}/[0]_{12}$	997 ± 125	$[0]_{16}/[0]_{16}$	42.04 ± 0.83

Table 5
G_{1c} and SLS results of 134 g/m2 LMPAEK panels (standard laminates).

Panel sequence	G_{1c} [J/m^2]	Crystallinity (%)	Voids (%)
$[+45, 0, -45, 90, -45, 0, 45, 0, 45, 0, -45, 90, -45, 0, 45]_s$	2164 ± 372	21.6 ± 1.1	1.4 ± 0.5
$[+45, 0, -45, 90, -45, 0, 45, 0, 45, 0, -45, 90, -45, 0, 45]_s$	2033 ± 158	20.4 ± 1.2	1.4 ± 0.3

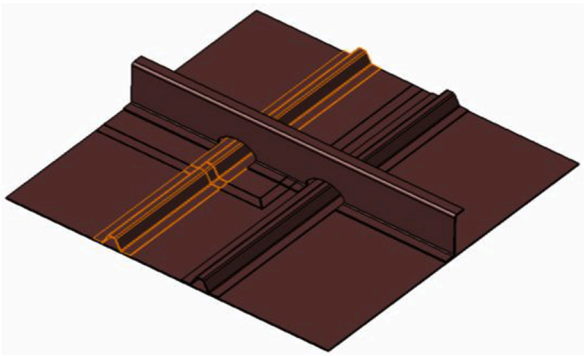

Fig. 14. Joggled omega stiffeners (For interpretation of the references to colour in this figure caption, the reader is referred to the web version of this paper).

Fig. 15. Straight omega stringer after trimming.

Fig. 16. Joggled omega stringer after trimming.

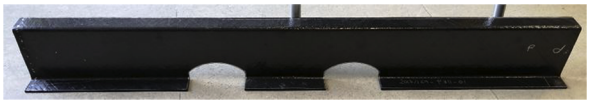

Fig. 17. Z-shaped frame after trimming.

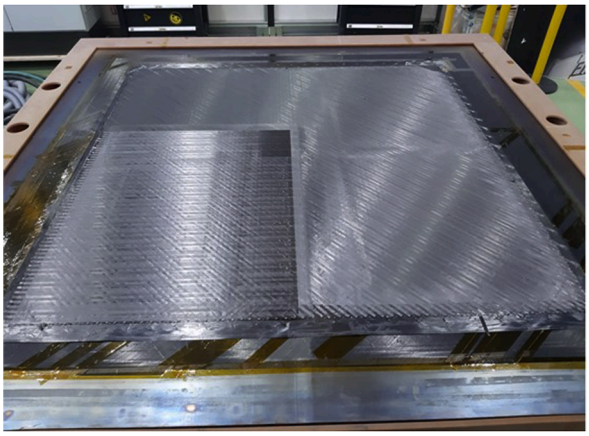

Fig. 18. Image of the skin and reinforced area (For interpretation of the references to colour in this figure caption, the reader is referred to the web version of this paper).

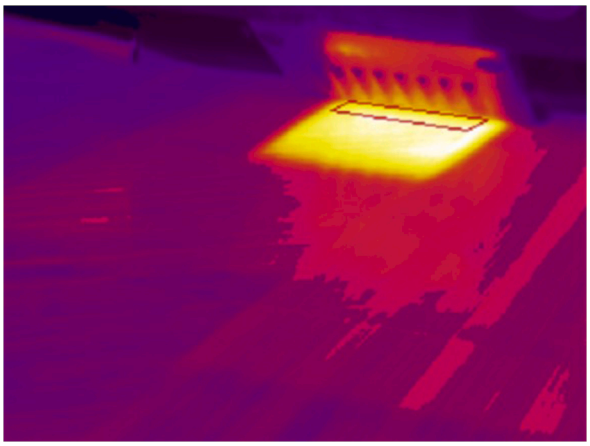

Fig. 19. Laser heating spot and control area (For interpretation of the references to colour in this figure caption, the reader is referred to the web version of this paper).

Table 6
Lamination parameters.

Parameter	Value	Unit
Head load	250	kgf
Nip point temperature	380	°C
Speed	1	m/min
Heating spot area	50 × 70	mm^2
Laser angle	70	°

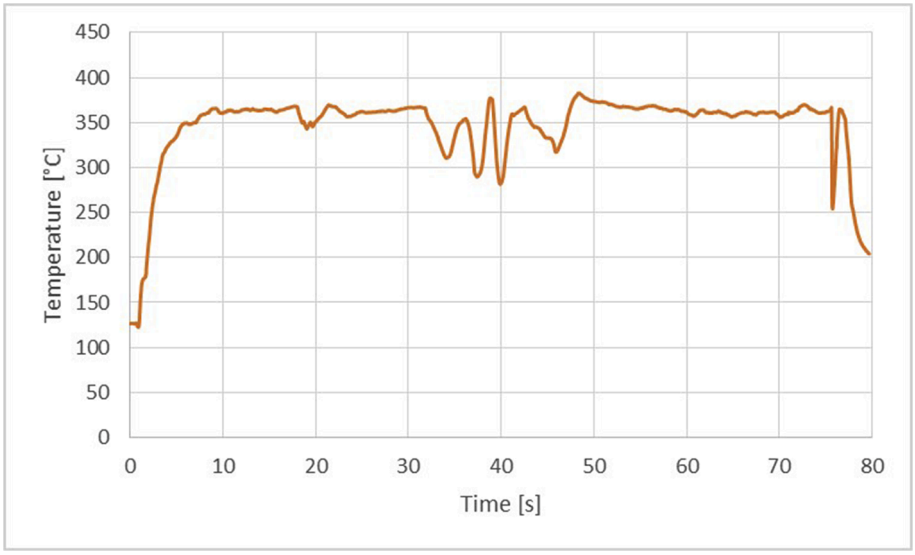

Fig. 20. Laying-up of second layer (passing over the frame).

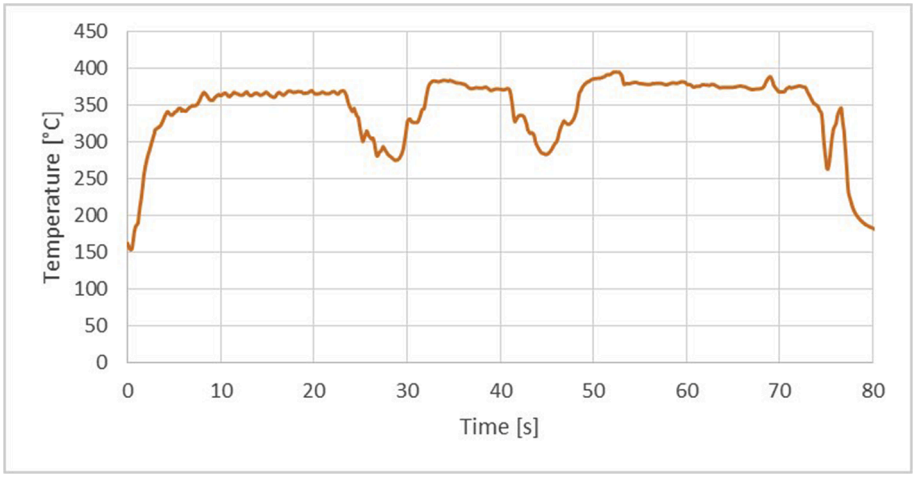

Fig. 21. Laying-up of fourth layer (passing over both stringers).

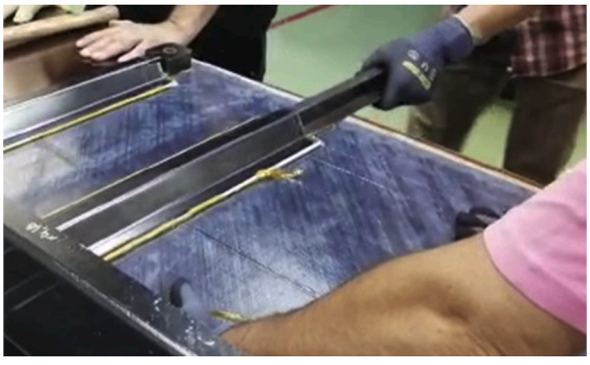

Fig. 22. Omega module extraction (For interpretation of the references to colour in this figure caption, the reader is referred to the web version of this paper).

gradients induced by the different thermal conductivity of these elements has a significant impact on polymer melting.

5.4. Demoulding

After lamination, the entire component (skin and stiffeners) was extracted from the tooling, along with the metallic modules. First, the metallic module associated with the frame was removed from the set; subsequently, the two-part split modules of the omega-stringers were removed from each tip, as shown in Fig. 22.

5.5. Dimensional inspection

The thickness of each stiffener was checked at different points along the length after the manufacturing process was completed (measuring with a caliper). On average, the measured thickness was 6% lesser than the nominal thickness.

Several factors were identified that may have impacted the thickness. First, the use of a hard tooling requires strict tolerances to achieve homogenous pressure distribution. Second, the low viscosity of the LMPAEK material increased the required cycle pressures, which caused the resin to ooze out (Fig. 23), thereby necessitating the use of retention systems. Oozing out was also checked by microscopic analysis.

Considering the skin, several measurements were recorded from different areas of the panel. On average, the measured thickness was 5% higher than the nominal thickness. Other studies have also reported similar effects. For example, Blanco [24] performed manufacturing trials using thermoplastic composites in the shape of commingled yarns and filament winding; the impacts of the heating source temperature and speed on the thickness of the final part were clarified. The higher the temperature, the lower the material viscosity, allowing more free movement under pressure. The higher the speed, the lower the duration spent under the compactor (or roller), thereby reducing the pressure profiles.

Considering the models that describe intimate contact and bonding among layers [25–27], bonding is directly linked to pressure and time. A reduction in the time–pressure profile could increase the number of voids among the layers, resulting in a higher thickness.

5.6. Microscopic inspection

Samples were cut from different areas, polished, and observed under a microscope. The samples included the skin, reinforced skin area, stringer–skin interface (Fig. 24), and frame–skin interface. As shown in Fig. 25, no voids were present at the stringer–skin interface. Although this does not guarantee a good degree of bonding, it is a significant achievement and a fulfilled requirement for a good mechanical response.

The skin was subjected to an in-depth microscopic analysis to determine the quality of lamination. It also exhibited a lack of defects.

5.7. Non-destructive inspection

An ultrasound-based (pulse echo technique) non-destructive inspection of each stiffener was performed after press forming. The skin–stiffeners assembly was also inspected after lamination to verify the quality of the entire skin and bonding lines.

The NDT inspection manifested that the part fulfils the quality criteria following aeronautic standard for thermoset and thermoplastic composite materials.

6. Conclusion

Press forming was used to manufacture high quality stiffeners for use in a subsequent assembly along with the skin. The thickness of the stiffeners exhibited deviations that can be overcome by improving the tooling tolerances, resin retention, and pressure distribution.

For future industrialisation, a more productive process, such as stamp forming, must be used to reduce the cycle time. Nevertheless, this study enabled the evaluation of the tooling equipment and the mechanical testing of the skin–stiffener interface, providing evidence for the possibilities of manufacturing thermoplastic composites.

Low-melting PAEK material exhibited good results with in-situ consolidation, which thus far has been focused on the use of PEEK or PEKK based composites.

A highly integrated reinforced demonstrator was manufactured by direct lamination of the skin on top of the stiffeners. Laser heating was a determining factor, not only in terms of the required temperature but also considering the heated areas. If the substrate is non-homogeneous (different kinds of materials, temperature values, and conductivities), the laser spot should be carefully guided and

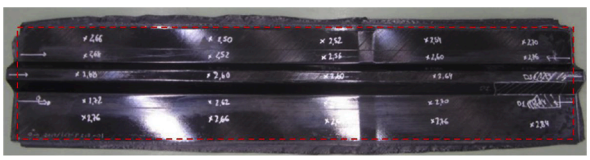

Fig. 23. Effect of resin oozing out.

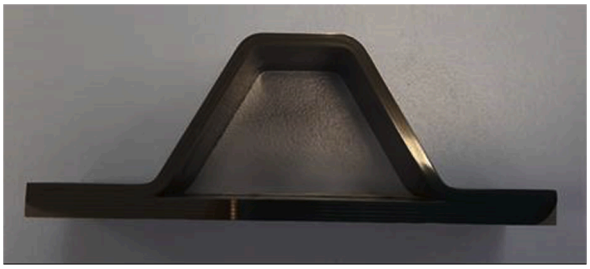

Fig. 24. Sample for microscopic inspection of the welding line.

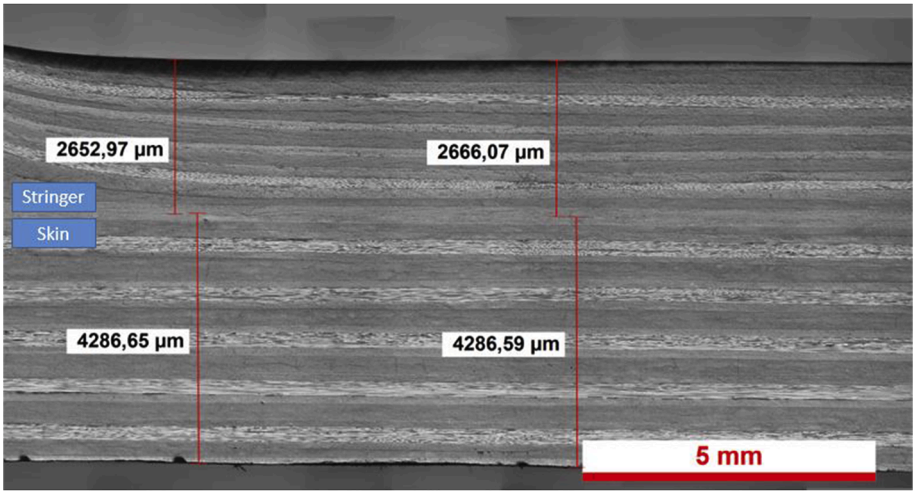

Fig. 25. Microscopic image of the interface between the skin and omega-shaped stringer (For interpretation of the references to colour in this figure caption, the reader is referred to the web version of this paper.

regulated. The development of a heating source with variable and independent spots for each laminated tow could improve the quality of the assembled part, allowing temperature control in specific areas (as achieved in Ref. [28]).

The parameter selection to manufacture the part was possible thanks to the previous experience of FIDAMC working with in-situ consolidation processes using other materials, although during this work, certain defects associated to the process were overcome. The warpage was avoided by the interaction of the stiffeners which reinforce the structure avoiding geometrical distortions. Steering defects, gaps and overlaps were avoided by tuning specific parameters, as laser turn on/off and several iterations of programming and testing lamination. Mechanical results obtained from flat panels and those resembling the adhesion skin-stringer manifest the fulfilment of the requirements for a piece of this characteristics.

The adhesion levels between the skin and stiffeners will be checked using the samples extracted from the flat demonstrator to generate a database of the mechanical performance for use in future studies (LPA level 3 testing of curved demo structure). This work is the prelude of subsequent activities in the frame of CS2 that will be published in future related articles, it tries to manifest the ability to generate a flat demonstrator for testing whose results will be used for design and latterly for manufacturing a curved demo, the final goal of the project.

Based on the information obtained from this study, a cost and time analysis should be performed. Coupled with the mechanical testing of the component, this analysis can be used to demonstrate the benefits of employing in-situ consolidation with thermoplastic composite materials for primary structures.

Funding

This work was supported by the Large Passenger Aircraft (LPA GAM 2019) project [grant number 807097]. The authors would like to thank the European Commission for their financial assistance and for promoting cooperation between research and industry across Europe.

References

[1] A. Hiken, The evolution of the composite fuselage: a manufacturing perspective, Int J Aerosp 10 (2) (2017) 77–91.

[2] S.L. Veldman, P. Kortbeek, P.C. Wölcken, R. Herrmann, J. Kos, I.F. Villegas, Development of a multifunctional fuselage demonstrator, in: Aerospace Europe Conference 2020, 2020. Bordeaux, France.
[3] J.W. van Ingen, Thermoplastic orthogrid fuselage shell, SAMPE J. 52 (5) (2016) 7–15.
[4] J.W. van Ingen, J. Waleson, A. Offringa, M. Chapman, Double curved thermoplastic orthogrid rear fuselage shell, in: SAMPE Europe Conference 19, Nantes, France, 2019, pp. 1–10.
[5] K.S. van Dooren, C. Bisagni, Design and analysis of thermoplastic welded stiffened panels in post-buckling, in: Proceedings of the American Society for Composites, Thirty-Sixth Technical Conference, 2021, pp. 406–417.
[6] S. Kothe, B. Diehl, D. Niermann, L. Chen, M. Wolf, W. Hintze, Automated assembly of thermoplastic fuselage structures for future aircrafts, in: B.A. Behrens, A. Brosius, W. Hintze, S. Ihlenfeldt, J.P. Wulfsberg (Eds.), Production at the Leading Edge of Technology. WGP 2020. Lecture Notes in Production Engineering, Springer, Berlin, Germany, 2020, pp. 467–475.
[7] P. Nijhuis, Thermoplastic Stiffened Wing Skin Made by Advanced Fibre Placement, 2009.
[8] K. Yassin, M. Hojjati, Processing of thermoplastic matrix composites through automated fiber placement and tape laying methods: a review, J. Thermoplast. Compos. Mater. 31 (12) (2018) 1676–1725.
[9] J. Weber, J. Schlimbach, Co-consolidation of CF/PEEK tape-preforms and CF/PEEK organo sheets to manufacture reinforcements in stamp-forming process, Adv. Manuf. Polym. Compos. Sci. 5 (4) (2019) 172–183.
[10] T.E. Saliba, D.P. Anderson, R.A. Servais, Process modeling of heat transfer and crystallisation in complex shapes thermoplastic composites, J. Thermoplast. Compos. Mater. 2 (2) (1989) 91–104.
[11] J. Reichardt, I. Baran, R. Akkerman, New analytical and numerical optical model for the laser assisted tape winding process, Compos. Appl. Sci. Manuf. 107 (2018) 647–656.
[12] I. Schiel, L. Raps, A.R. Chadwick, I. Schmidt, M. Simone, S. Nowotny, An investigation of in-situ AFP process parameters using CF/LM-PAEK, Adv. Manuf. Polym. Compos. Sci. 6 (4) (2020) 191–197.
[13] S. Maison, et al., U.S. Patent No. 6,613,258, U.S. Patent and Trademark Office, Washington, DC, 2003.
[14] F. Rodríguez-Lence, M. Zuazo, S. Calvo, In-situ consolidation of PEEK composites by automated placement technologies, in: Proceedings of the 20th International Conference on Composite Materials, 2015. Copenhagen, Denmark.
[15] M. Zuazo, F. Chamorro, V. Garcia-Martinez, S. Calvo, E. Lorenzo-Villafranca, One shot manufacturing of a highly integrated structure by automatic lamination with thermoplastic composite materials, AEMAC 4 (3) (2020) 103–106.
[16] A.K. Bandaru, G.J. Clancy, D. Peeters, R. O'Higgins, P.M. Weaver, Interface Characterisation of Thermoplastic skin-stiffener composite manufactured using laser-assisted tape placement. In: 2018 AIAA/ASCE/AHS/ASC Structures, Structural Dynamics, and Materials Conference, Kissimmee, USA, 2018, p. 481.
[17] J. Veijer, Analytical Model of a Mold Dependent Production Line: Applied to Future thermoplastic skin panel production for Gulfstream G650 tail wings. Master's Thesis, University of Twente, 2015.
[18] MIL-HDBK-17, Composite Materials Handbook. Polymer Matrix Composites Materials Usage, Design, and Analysis, 2002.
[19] M. Brzeski, R. Holschuh, R. Scheldjewski, Effect of tool temperature on laminate properties during in situ consolidation placement process, in: International SAMPE Symposium and Exhibition. 2010. p.17–20. ISO 11357-3: 2018(E). Plastics — Differential Scanning Calorimetry (DSC) — Part 3: Determination of Temperature and Enthalpy of Melting and Crystallisation, 2018.
[20] Plastics — Differential Scanning Calorimetry (DSC) — Part 3: Determination of Temperature and Enthalpy of Melting and Crystallisation, 2018.
[21] UNE-EN 2564, Aerospace Series - Carbon Fibre Laminates - Determination of the Fibre, Resin and Void Contents. 2018, 2018.
[22] AITM 4-0005. Macroscopic and Microscopic Examination of Fiber Reinforced Plastics.
[23] F. Shadmehri, S.V. Hoa, J. Fortin-Simpson, H. Ghayoor, Effect of in situ treatment on the quality of flat thermoplastic composite plates made by automated fiber placement (AFP), Adv. Manuf. Polym. Compos. Sci. 4 (2) (2018) 41–47.
[24] J.M. Blanco, Adaptation and Study of a Filament Winding Machine for In-Situ Consolidation of Thermoplastic Composites, Master's Thesis, ETH, Zurich, 2014.
[25] W.I. Lee, G.S. Springer, A model of the manufacturing process of thermoplastic matrix composites, J. Compos. Mater. 21 (11) (1987) 1017–1055.
[26] A.C. Loos, P.H. Dara, Processing of thermoplastic matrix composites, in: D.O. Thompson, D.E. Chimenti (Eds.), Review of Progress in Quantitative Nondestructive Evaluation, vol. 6A, Springer, Boston, MA, 1987, pp. 1257–1265.
[27] R. Pitchumani, S. Ranganathan, R.C. Don, J.W. Gillespie Jr., M.A. Lamontia, Analysis of transport phenomena governing interfacial bonding and void dynamics during thermoplastic tow-placement, Int. J. Heat Mass Tran. 39 (9) (1996) 1883–1897.
[28] M. Assadi, T. Field, AFP processing of dry fiber carbon materials (DFP) for improved rates and reliability, SAE Int J Adv Curr Prac Mobil 2 (3) (2020) 1196–1201.